Cancer Research

Identification of RNA-Binding Protein LARP4B as a Tumor Suppressor in Glioma

Hideto Koso[1], Hungtsung Yi[1], Paul Sheridan[2], Satoru Miyano[2], Yasushi Ino[3], Tomoki Todo[3], and Sumiko Watanabe[1]

Abstract

Transposon-based insertional mutagenesis is a valuable method for conducting unbiased forward genetic screens to identify cancer genes in mice. We used this system to elucidate factors involved in the malignant transformation of neural stem cells into glioma-initiating cells. We identified an RNA-binding protein, La-related protein 4b (LARP4B), as a candidate tumor-suppressor gene in glioma. *LARP4B* expression was consistently decreased in human glioma stem cells and cell lines compared with normal neural stem cells. Moreover, heterozygous deletion of *LARP4B* was detected in nearly 80% of glioblastomas in The Cancer Genome Atlas database. *LARP4B* loss was also associated with low expression and poor patient survival. Overexpression of LARP4B in glioma cell lines strongly inhibited proliferation by inducing mitotic arrest and apoptosis in four of six lines as well as in two patient-derived glioma stem cell populations. The expression levels of *CDKN1A* and *BAX* were also upregulated upon LARP4B overexpression, and the growth-inhibitory effects were partially dependent on p53 (TP53) activity in cells expressing wild-type, but not mutant, p53. We further found that the La module, which is responsible for the RNA chaperone activity of LARP4B, was important for the growth-suppressive effect and was associated with *BAX* mRNA. Finally, LARP4B depletion in p53 and Nf1-deficient mouse primary astrocytes promoted cell proliferation and led to increased tumor size and invasiveness in xenograft and orthotopic models. These data provide strong evidence that LARP4B serves as a tumor-suppressor gene in glioma, encouraging further exploration of the RNA targets potentially involved in LARP4B-mediatd growth inhibition. *Cancer Res; 76(8); 2254–64. ©2016 AACR.*

Introduction

Glioblastoma is the most common form of malignant brain cancer in adults. Patients with glioblastoma invariably have a bad prognosis, with a mean survival of around 1 year (1). Thus, more studies are needed to better combat this disease. Genome sequencing has revealed a plethora of mutations in glioblastoma (2); however, the pathologic relevance of these mutations is unclear. Transposon-based insertional mutagenesis is useful as it allows for an unbiased forward genetic screen for cancer genes in mice (3, 4), thereby providing a functional readout to complement cancer genome-sequencing studies. We used transposon mutagenesis to better understand the genes and pathways that are able to transform neural stem cells (NSC) into glioma-initiating cells (5), and identified La-related protein 4b (*Larp4b*) as a candidate tumor-suppressor gene in glioblastoma.

The La-related proteins (LARP) are characterized by the presence of a La motif (LaM), which is a highly conserved domain similar in structure to the winged-helix motif commonly found in DNA-binding transcriptional factors (6). The La motif is immediately followed by one or several RNA-recognition motifs (RRM), and this tandem arrangement is known as the La module. The functions of the La module have been best studied in the genuine La proteins (7). The genuine La protein La module binds to 3′ oligo (uridylic acid) stretches (UUU-3′OH), which are commonly found in newly synthesized RNA polymerase III transcripts, such as tRNA and 5S rRNA precursors. La engagement is thought to protect RNA trailers from 3′ exonuclease digestion and to assist their folding via its RNA chaperone activity.

Seven different LARPs have been identified in humans (*LARP1*, *1B*, *4*, *4B*, *6*, and *7*) based on their homology with genuine La proteins (8). However, the functions and binding modes of the La module in LARPs are not well understood. One of the best-characterized human LARPs is LARP7. By stabilizing 7SK RNA, LARP7 inhibits the cyclin-dependent kinase (CDK) activity of p-TEFb (9, 10), and functions as a tumor-suppressor gene in several types of human cancer (11, 12). LARP4B is a cytosolic protein, which interacts with the cytosolic polyA-binding protein 1 (PABPC1) and the receptor for activated C kinase (RACK1), a component of the 40S ribosomal subunit (13). Schaffler and colleagues also showed that overexpression of *LARP4B* stimulated protein synthesis, whereas a knockdown of *LARP4B* impaired translation of a large number of mRNAs, suggesting a stimulatory role for LARP4B in translation (13). In the present study, we identified LARP4B as a potential tumor-suppressor gene in gliomas. An analysis of cancer database information suggested that LARP4B participates in the pathogenesis of human glioma, and cellular analyses revealed its function as a tumor suppressor.

[1]Division of Molecular and Developmental Biology, The Institute of Medical Science, The University of Tokyo, Tokyo, Japan. [2]Laboratory of DNA Information Analysis, Human Genome Center, The Institute of Medical Science, The University of Tokyo, Tokyo, Japan. [3]Division of Innovative Cancer Therapy, The Institute of Medical Science, The University of Tokyo, Tokyo, Japan.

Note: Supplementary data for this article are available at Cancer Research Online (http://cancerres.aacrjournals.org/).

H. Koso and H. Yi contributed equally to this article.

Corresponding Author: Sumiko Watanabe, Institute of Medical Science, The University of Tokyo, 4-6-1 Shirokanedai, Minato-ku, Tokyo 108-8639, Japan. Phone: +81-3-5449-5664; Fax: 81-3-5449-5474; E-mail: sumiko@ims.u-tokyo.ac.jp

doi: 10.1158/0008-5472.CAN-15-2308

AACR

Materials and Methods

Retroviral expression vectors

pMXs-IRES-Puro (pMXs-IP; Cell Biolabs, Inc.) and MSCV-LTRmiR30-PIG (LMP; Thermo Scientific) were used for the overexpression and knockdown experiments, respectively. Details on the vector construction strategies are described in Supplementary Materials and Methods.

Glioma cell lines

Five human glioma cell lines were obtained from the ATCC: U-87MG (ATCC HTB-14), U-118MG (ATCC HTB-15), U-138MG (ATCC HTB-16), T98G (ATCC CRL-1690), and A172 (ATCC CRL-1620). U-251MG was obtained from the JCRB Cell Bank (IFO50288). All cell lines tested negative for *mycoplasma* contamination. The lines were authenticated by standard morphologic examination using microscopy. The glioma cell lines were cultured in DMEM containing 10% FBS and penicillin–streptomycin.

Glioma stem cells

Information regarding the patient-derived glioma stem cells (TGS-01, TGS-02, and TGS-04; ref.14) is provided in Supplementary Table S1. Glioma stem cells were cultured in DMEM/F12 supplemented with B27 (Invitrogen), 20 ng/mL EGF, and 20 ng/mL bFGF (both from PeproTech).

Preparation of primary astrocytes

Primary astrocytes were harvested from the brains of neonatal C57BL6/J mice as described previously (15). After 1 to 2 weeks, growing cells were retrovirally transduced with dominant-negative p53 (p53DN; ref.15) and used as immortalized astrocytes.

Retroviral infection

Retrovirus was generated with Platinum-A packaging cells (Cell Biolabs, Inc.) and used to infect target cells as described previously (5). Infected cells were selected with puromycin (2 μg/mL) for 2 days and used for proliferation assays. Details on the method used to serially infect target cells with different retroviruses are provided in Supplementary Materials and Methods.

Cell proliferation assay

LARP4B-transduced or control cells (5×10^4) were plated in 6-well plates in triplicate. The total number of cells was counted on day 5, and the fold change was calculated. Viable cell counting was performed using the Trypan Blue exclusion method.

Western blot analysis

HEK293T cells (ATCC) were transfected using GeneJuice transfection reagent (Millipore). After 48 hours, the transfected cells were collected and used for Western blotting. Primary antibodies against HA (Covance), actin (Sigma), Larp4b (Abcam), and horseradish peroxidase–linked secondary antibodies (GE Healthcare) were used. Band intensities were quantified using ImageJ software.

Real-time PCR analysis

To analyze the expression levels of the candidate genes in Table 1, total RNA was extracted from NSCs, glioma stem cells, and cell lines using Sepazol (Nacalai Tesque, Inc.). cDNA was synthesized with ReverTra Ace (Toyobo), and qPCR was performed using TaqMan assays (Invitrogen; Supplementary Table S2). All other qPCR experiments were performed with the primers shown in Supplementary Table S3 using the LightCycler 96

Table 1. Genomic alterations in candidate tumor-suppressor genes in human glioblastoma

Gene	%Homo_Del[a]	%Hetero_Del[b]	%Diploid[c]	%Low_Amp[d]	%High_Amp[e]	%Mut[f]	Expression *P* val (adjusted)[g]	Cox *P* val (adjusted)[h]
PTEN	9.7	79.4	10.6	0.2	0.2	34.3	N/A	4.5E−03
VTI1A	0.2	88.4	10.9	0.3	0.2	0.0	4.0E−05	1.1E−02
DDX50	0.3	86.8	12.5	0.3	0.0	0.0	2.6E−04	1.5E−03
MLLT10	0.3	82.1	14.7	2.1	0.7	0.0	8.3E−04	4.0E−04
LARP4B	0.7	80.9	15.6	2.1	0.7	0.4	<1.0E−05	1.1E−03
IFT74	6.6	48.4	39.7	5.2	0.2	0.4	<1.0E−05	0.99
BNC2	1.6	48.9	42.6	5.9	1.0	1.6	5.8E−02	0.95
MPDZ	1.7	45.6	45.2	6.9	0.5	0.4	<1.0E−05	0.55
UHRF2	1.6	40.7	49.9	7.5	0.3	0.4	<1.0E−05	0.97
ATXN10	0.5	35.9	57.9	5.5	0.2	0.0	<1.0E−05	0.99
QKI	2.6	29.8	63.3	4.3	0.0	2.0	<1.0E−05	0.38
MNAT1	0.5	29.1	66.2	4.2	0.0	0.0	<1.0E−05	0.99
ARID1B	0.7	28.1	67.1	4.0	0.2	0.4	<1.0E−05	0.40
MAPK1	0.2	30.3	62.7	6.4	0.3	0.8	N/A	0.90
RCOR1	0.3	27.4	67.1	5.0	0.2	0.4	<1.0E−05	0.99
TRAF3	0.3	27.2	67.2	5.0	0.2	0.0	N/A	0.99
CYFIP1	0.0	21.1	74.7	4.2	0.0	0.0	1.8E−02	0.72

Abbreviation: N/A, data not available in the TCGA dataset.

[a–f]The percentage (%) of tumors with homozygous deletion (Homo_Del), heterozygous deletions (Hetero_Del), diploid, low amplification (Low_Amp), high amplification (High_Amp), and somatic mutation (Mut). The total number of tumor samples analyzed for copy-number alterations and mutations are 565 and 283, respectively.

[g]Correlation between copy-number alterations and expression changes was analyzed between those tumor samples in which it is deleted versus amplified/normal ones. *P* values were calculated according to the two-sample *t* test and adjusted for multiple testing using the Benjamini–Hochberg method in the R project function p.adjust. The total number of tumor samples analyzed for expression changes is 147.

[h]Correlation between copy-number alterations and clinical status (Kaplan–Meier survival) was analyzed between those tumor samples in which it is deleted versus amplified/normal ones. *P* values were calculated according to the Cox regression analysis and adjusted for multiple testing using the Benjamini–Hochberg method in the R project function p.adjust. The total number of tumor samples analyzed for Cox regression analysis is 565.

System (Roche). Expression profiling of the glioma stem cells was performed with institutional approval (IMSUT).

Immunohistochemical analysis

Actin staining was performed with rhodamine-phalloidin (Wako). For analysis of the brain, perfusion fixation was performed prior to dissection, and the brain was fixed in 4% PFA. For immunostaining, sections were incubated with primary antibodies against GFP (Abcam), S100b (Sigma), Gfap (Sigma), or CD31 (BD), and then incubated with the appropriate secondary antibodies. EdU staining was performed using Click-iT Assay Kits (Invitrogen) according to the manufacturer's protocol. Nuclei were counterstained with DAPI. Stained cells were observed with an inverted fluorescence light microscope (Zeiss), and images were acquired with AxioImager software.

Cell-cycle analysis

Cells were harvested on day 5 after plating, fixed in 70% ethanol, and incubated with 33 μg/mL ribonuclease A. Next, the cells were resuspended in 1% propidium iodide (PI) to label the DNA. DNA content was measured using a FACSCalibur instrument (BD) and analyzed with FlowJo software.

Cell apoptosis analysis

Cells were harvested at day 5 after plating and stained with Annexin V–FITC (BioVision) and PI. Stained cells were analyzed by using FACSCalibur (BD), and the data were analyzed with CellQuest software.

RNA immunoprecipitation-PCR

Cells were harvested 2 days after plating and lysed as described previously (16). Immunoprecipitation was performed using anti-HA magnetic beads (MBL). Coprecipitated RNA was isolated from the beads and input control using phenol extraction. cDNA was generated, and qPCR was performed with the primers listed in Supplementary Table S3.

Animal experiments

A total of 5×10^6 of immortalized astrocytes transduced with either shRNA against luciferase (shLuc) or *Larp4b* were injected subcutaneously into the flank of three recipient C57BL6/J mice. The size of each tumor was measured every week until week 9, and the tumor volume was estimated by multiplying the length, width, and height. For intracranial transplantation, 2×10^5 cells were injected into the striatum of C57BL6/J mice on postnatal day 7 (P7). After 2 or 8 weeks, histologic analyses were performed. EdU (50 mg/kg) was intraperitoneally administered for 2 consecutive days before sacrifice. All procedures were performed with institutional approval (IMSUT).

Analysis of The Cancer Genome Atlas datasets

A total of 565 glioblastoma primary tumor cases from The Cancer Genome Atlas (TCGA) were analyzed, all of which had genome-wide copy-number profiling and clinical data; of these, 283 cases had associated exome sequencing data, 73 had DNA methylation data, and 147 had mRNA expression data (Broad Institute analysis run from December 17, 2014; doi:10.7908/C10V8BNC). Details on the methods for data analysis are given in Supplementary Materials and Methods.

Results

LARP4B is a candidate tumor-suppressor gene in glioma

We previously identified more than 100 candidate cancer genes for glioma using transposon-based insertional mutagenesis (5). Among these, we focused on 88 genes predicted to function as tumor-suppressor genes based on transposon insertion patterns (Supplementary Table S4). To investigate the possibility that these genes function as tumor suppressors in human glioma, we first examined DNA copy-number alterations using 577 human glioblastoma samples in the TCGA database. Copy-number loss was more frequently observed than copy-number gain for 54 genes (Supplementary Table S4). A total of 17 genes had copy-number loss in more than 20% of cases (Table 1), and these genes included well-established tumor-suppressor genes such as *PTEN and QKI* (17, 18), as well as genes that had been previously unreported as tumor suppressors. Notably, four genes (*VTI1A*, *DDX50*, *MLLT10*, and *LARP4B*) showed heterozygous deletion in more than 80% of glioblastoma samples (Table 1, %Hetero_Del). We next analyzed the relationship between copy-number loss and gene expression levels. Tumors with copy-number loss had much lower expression levels of these genes than did tumors with no copy loss (Table 1; Expression p-val). We also investigated the correlation between copy-number changes and patient survival, and found that a low copy number of five genes (*PTEN*, *VTI1A*, *DDX50*, *MLLT10*, and *LARP4B*) predicted poor patient survival (Table 1; Cox p-val). We next compared the expression levels of the 17 genes in Table 1 between normal NSCs and glioma. We used two NSC lines differentiated from two human iPS cells (tkCB_Sev9 and tkDA_3-4; ref.19) and one commercially available NSC line derived from an embryonic stem cell (ES) line. We also used three glioma stem cells (14) and six glioma cell lines. Real-time PCR analysis revealed that the expression levels of 15 genes were significantly decreased in glioma cells compared with normal NSCs (Fig. 1A and B), consistent with their putative tumor-suppressor functions.

We next focused on human *LARP4B*, which is located at 10p15.3 and is frequently deleted in glioblastoma (Fig. 1C) because its role in glioma has not yet been reported. Transposon insertions in the *Larp4b* gene locus were distributed throughout the gene, with little orientation bias (Fig. 1D), suggesting a tumor-suppressor role for *Larp4b*. In addition, when we looked at the TCGA database, heterozygous deletion of *LARP4B* was found in 80.9% of glioblastoma cases, whereas homozygous deletion was only found in 0.7% (Table 1). DNA copy-number status was correlated with *LARP4B* expression levels in glioblastoma samples (Fig. 1E). Furthermore, *LARP4B* loss was inversely correlated with patient survival (Fig. 1G), indicating that decreased *LARP4B* expression is a negative prognostic factor for human glioblastoma patients. Analysis of the methylation status of the *LARP4B* gene locus using the TCGA dataset (2) revealed that *LARP4B* was methylated in all of the 59 tumors with heterozygous *LARP4B* deletion had *LARP4B* DNA methylation, suggesting that the remaining allele may be transcriptionally silenced. An analysis of low-grade glioma samples in the TCGA database (Supplementary Table S5) also revealed that *LARP4B* loss was correlated with decreased expression and poor patient survival in low-grade glioma (Fig. 1F and H). Other LARP family genes (*LARP1*, *1B*, *4*, *6*, and *7*) were not significantly downregulated in glioma compared with NSCs (Supplementary Fig. S1A and S1B). These LARP family genes are mostly (~80%) diploid in glioblastoma

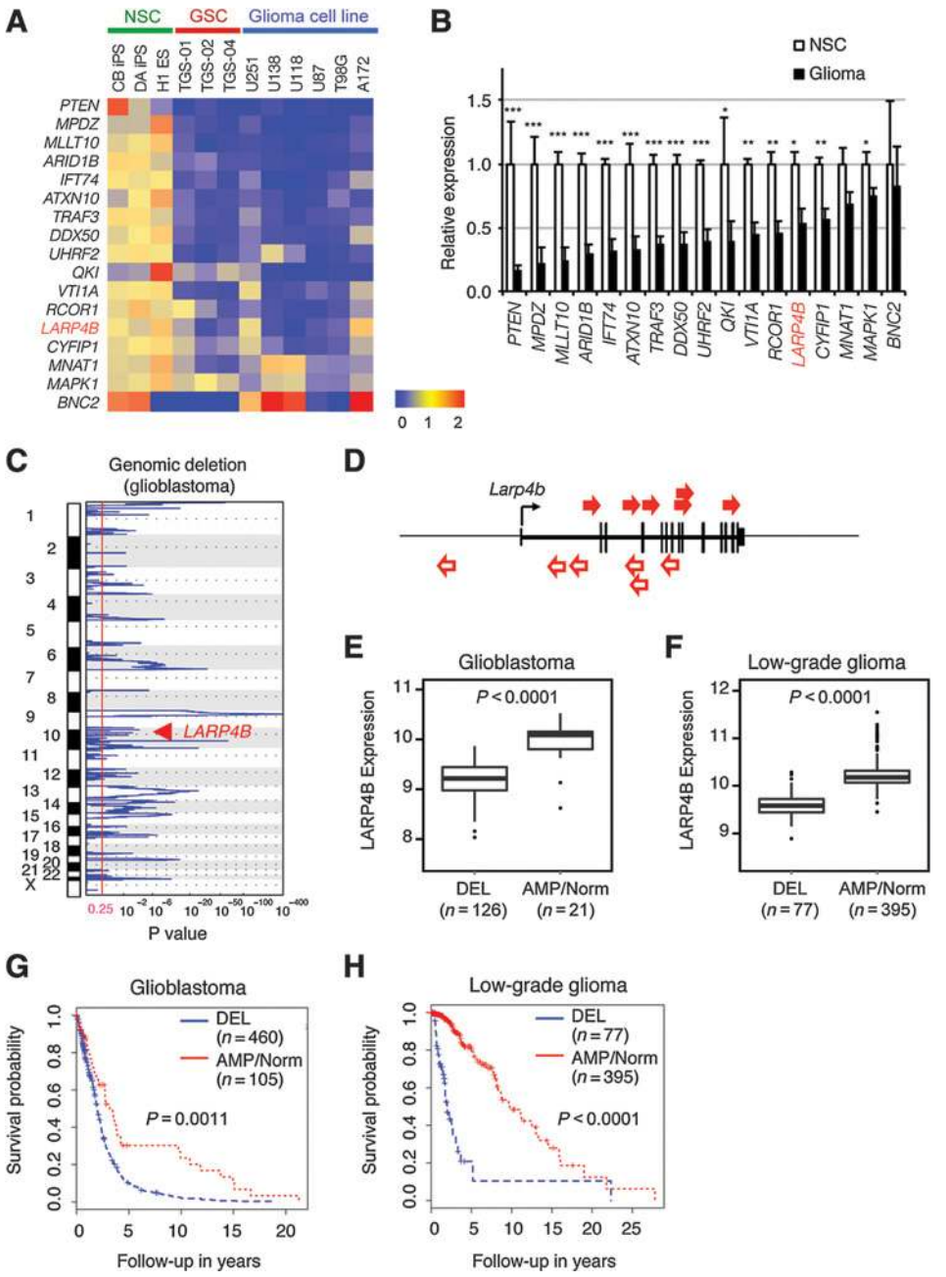

Figure 1.
Larp4b is a tumor-suppressor candidate in glioma. A and B, expression levels of candidate tumor-suppressor genes in Table 1. Expression levels are visualized in a heatmap (A), and compared between three NSCs and nine glioma samples (i.e. glioma stem cells and glioma cell lines; B). Data represent mean ± SEM. Student *t* test, *, $P < 0.05$; **, $P < 0.01$; ***, $P < 0.001$. C, *LARP4B* gene locus is located within the regions deleted in glioblastoma in the TCGA dataset. D, transposon insertions in the *Larp4b* gene locus are located in the sense (red arrows) or antisense orientations (white arrows) relative to transcription. E and F, the mRNA expression level of *LARP4B* is significantly decreased in those tumor samples in which it is deleted (DEL) compared with those with amplification (AMP) or normal (Norm) in glioblastoma (E) and low-grade glioma (F; $P < 0.0001$ according to a two sample *t* test). Relative expression levels are shown in $\log_2$ scale. G and H, Kaplan–Meier curves comparing overall survival of patients with *LARP4B* deletion (DEL) and amplification/normal (AMP/Norm) copy-number status in glioblastoma (G) and low-grade glioma (H). *P* values were calculated according to the Cox regression analysis and adjusted for multiple testing.

(Supplementary Table S6 and Supplementary Fig. S1C), and copy-number losses of these genes were not correlated with poor patient survival (Supplementary Fig. S1D). These data are consistent with the hypothesis that *LARP4B* serves as a tumor suppressor in human glioma.

LARP4B overexpression suppressed proliferation of glioma cell lines

To further investigate the tumor-suppressor function of *LARP4B*, we first examined whether transduction of *LARP4B* suppresses glioma cell growth by overexpressing *LARP4B* in human glioma cell lines. We generated an N-terminal HA-tagged LARP4B (Fig. 2A and B). We then retrovirally transduced either HA-LARP4B or the empty vector control into the glioma cell lines. The same number of infected cells was plated, and the cell number was determined on day 5. The number of control U87MG glioma cells increased continuously, resulting in a nearly 10-fold increase in total cell number (Fig. 2C and D; Supplementary Fig. S2A). In sharp contrast, proliferation of U87MG cells transduced with HA-LARP4B was greatly suppressed; the total cell number remained almost equal to the initial number (Fig. 2C and D). Similar growth suppression was observed for three other glioma cell lines, U87MG, U118MG, and A172, and two glioma stem cells, TGS-01 and TGS-04 (Fig. 2C and D; Supplementary Fig. S2A and S2B).

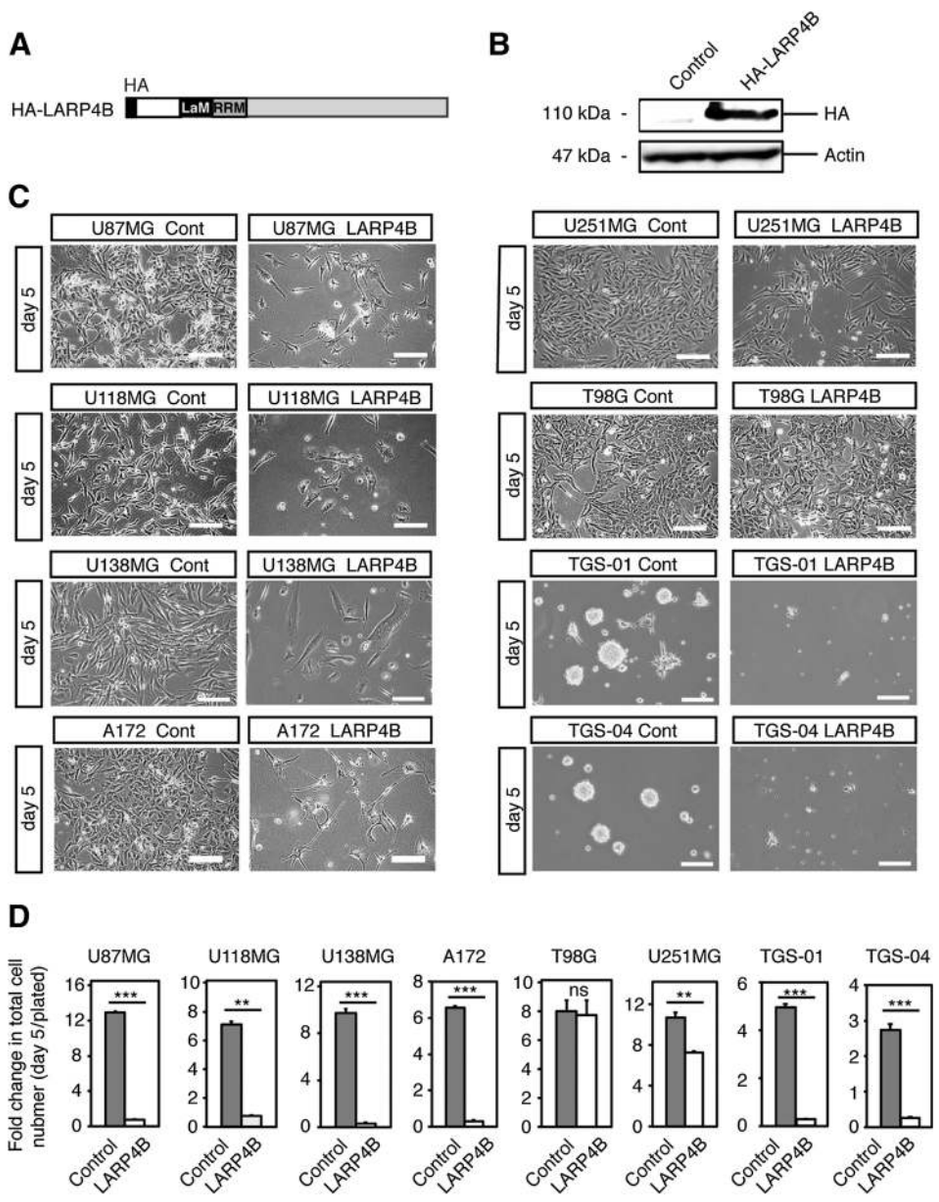

Figure 2.
LARP4B overexpression suppresses glioma cell growth. A, schematic drawing of HA-tagged LARP4B. LaM, La motif; RRM, RNA recognition motif. B, Western blot analysis of HA-LARP4B expression in HEK293T cells. C, glioma cells were retrovirally transduced with HA-LARP4B (LARP4B) or the vector control (Cont) and used for proliferation assays. The same number of infected cells was plated (day 0), and the morphology of the cells was observed on day 5. Bars, 200 μm. D, the fold change was calculated on day 5. Data represent mean ± SEM ($n = 3$ per group). Student t test, **, $P < 0.01$; ***, $P < 0.001$. Data are representative of two independent experiments.

However, such growth suppression was moderate for U251MG glioma cells, and T98G glioma cells continued to proliferate even after the transduction of LARP4B (Fig. 2C and D), indicating that the growth-suppressive effect of LARP4B is cell-line dependent.

LARP4B suppressed glioma cell growth by inducing mitotic arrest and apoptosis

The strong growth suppression of glioma cells by LARP4B suggested that glioma cells may have entered senescence after LARP4B transduction. One of the cardinal features of the senescent phenotype is a change in cellular morphology (20). Actin staining of the glioma cell lines in which *LARP4B* suppressed cell growth confirmed a flat and enlarged morphology (Fig. 3A). Notably, LARP4B overexpression increased the number of multi-nucleated cells in the U138MG cell line (Control: 5.8%, LARP4B: 30.1%, $P < 0.001$; Fisher exact test), suggesting that mitosis was deregulated by LARP4B. The proportion of multi-nucleated cells was not significantly altered in other lines. We next performed cell-cycle analysis (Gating strategies are shown in Supplementary Fig. S3A). The proportion of cells in the G_2–M phase was significantly increased by LARP4B overexpression in U87MG, U118MG, and U138MG glioma cell lines (Fig. 3B and D). Hyper-diploid cells were increased in U87MG by LARP4B (Fig. 3B and E), suggesting a premature exit from mitosis (21). Annexin V and PI staining showed that the fraction of Annexin V–positive and PI-negative apoptotic cells increased in three cell lines (U87MG, U118MG, and A172; Fig. 3C and F; gating strategies are shown in Supplementary Fig. S3B). Taken together, these data

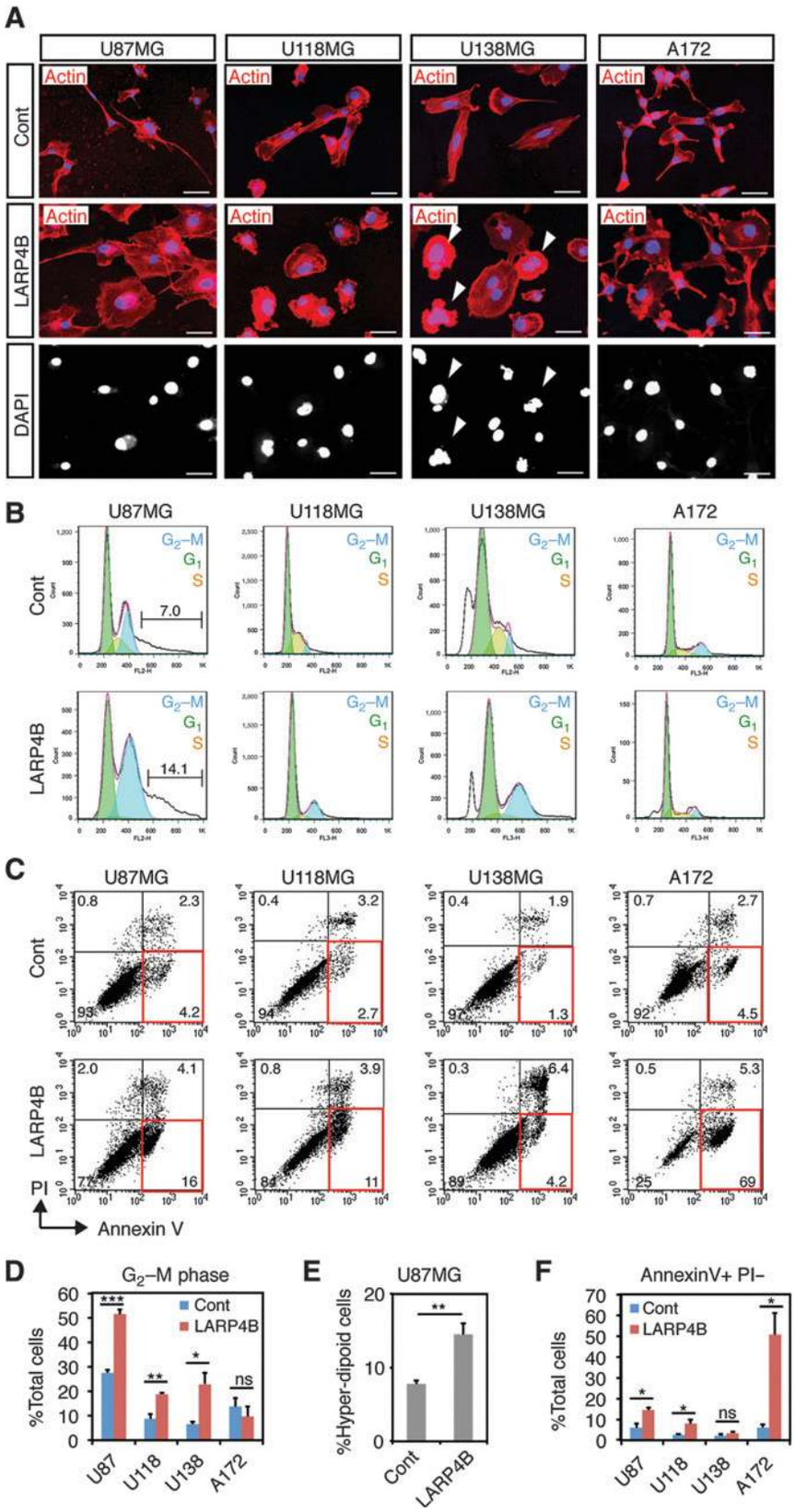

Figure 3.
LARP4B overexpression induces mitotic arrest and apoptosis of glioma cell lines. A, glioma cell lines transduced with HA-LARP4B were stained with rhodamine–phalloidin to visualize actin filaments. Arrowheads, multinucleated cells. Scale bars, 50 μm. B, cell-cycle analysis. Green, yellow, and blue histograms indicate G_1, S, and G_2–M phases of the cell cycle, respectively. Percentage of hyper-diploid cells is indicated in U87MG. C, analysis of apoptosis. Horizontal and vertical axes represent Annexin V expression and PI staining, respectively. D, the fractions of cells in the G_2–M phase are shown for control and LARP4B-transfected glioma cells. E, percentage of hyper-diploid cells in U87MG cells (B). F, the fractions of apoptotic cells (red squares in C) are shown for control and LARP4B-transfected glioma cells. Data represent mean ± SEM ($n = 3$ per group). Student t test, *, $P < 0.05$; **, $P < 0.01$; ***, $P < 0.001$. Data are representative of two independent experiments. Gating strategies are shown in Supplementary Fig. S3A and S3B.

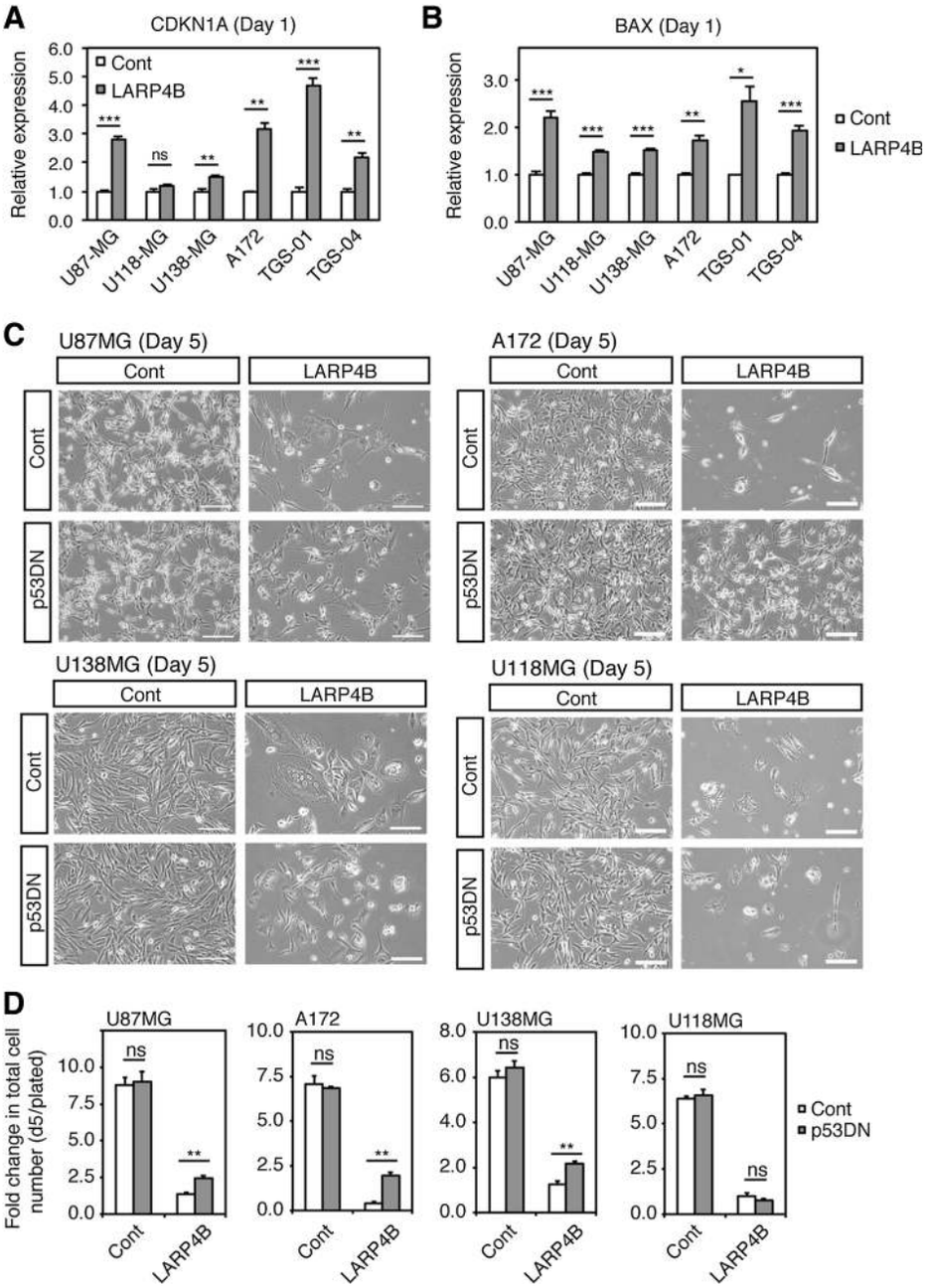

Figure 4.
p53 activity is partially required for the growth suppression of LARP4B. A and B, *CDKN1A* and *BAX* expression levels were analyzed on day 1. *GAPDH* was used as a normalization control. C and D, glioma cell lines transduced with either p53DN or the vector control were then transduced with either HA-LARP4B or the vector control. The morphology of the cells was observed on day 5 (C). Scale bars, 200 μm. The fold change was calculated on day 5 (D). Data represent mean ± SEM ($n = 3$ per group). Student t test, *, $P < 0.05$; **, $P < 0.01$; ***, $P < 0.001$. Data are representative of two independent experiments.

indicate that LARP4B suppressed glioma cell growth by inducing mitotic arrest and apoptosis.

p53 activity is partially required for LARP4B-mediated growth suppression

We next investigated the molecular mechanisms involved in LARP4B-mediated growth suppression. Mammalian CDK activity is essential for driving cell-cycle phases, and CDK activity is regulated by two families of inhibitors: INK4 proteins and the Cip and Kip family proteins (22). We first examined the expression of all INK4 genes and all Cip and Kip family genes in glioma cells transduced with *LARP4B*. We found that *CDKN1A* (also known as $p21^{CIP1}$) was upregulated in three of four glioma cell lines and two glioma stem cells after *LARP4B* transduction (Fig. 4A); however, the expression of other CDK inhibitors was not affected. In addition to mitotic arrest, LARP4B induced apoptosis in glioma cell lines. Apoptotic cell death is regulated by proapoptotic Bcl2 family members: *BAX* and its close relative *BAK1* (23). qPCR analysis revealed that *BAX* expression was significantly increased in all glioma cell lines and stem cells transduced with *LARP4B* (Fig. 4B). Cell-cycle arrest and apoptosis are often regulated by the activation of the p53 pathway in many types of cancer, and *CDKN1A* and *BAX* are both target genes of the p53 transcriptional factor (24), raising the possibility that p53

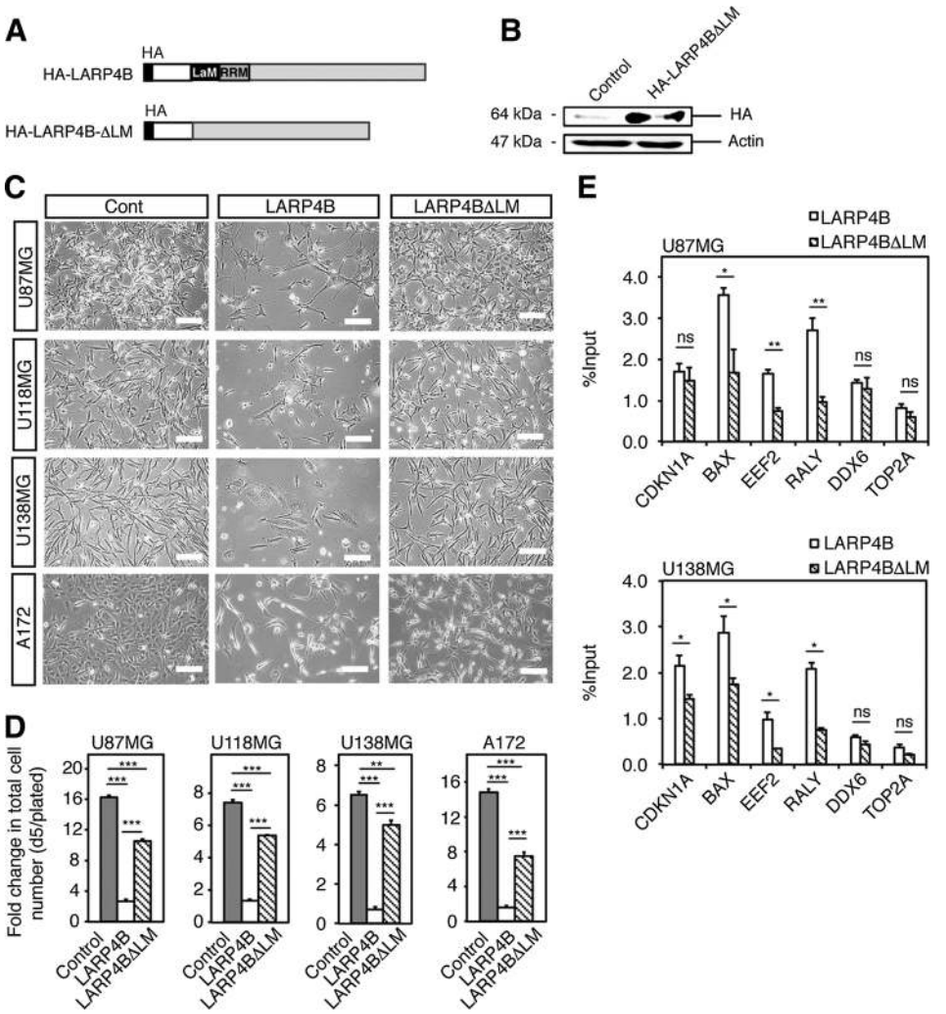

Figure 5.
The RNA-binding ability of LARP4B contributes to its growth-inhibitory function. A, schematic drawing of HA-tagged LARP4BΔLM. LaM, La motif; RRM, RNA recognition motif. B, Western blot analysis of HA-LARP4BΔLM expression in HEK293T cells. C, glioma cell lines were retrovirally transduced with either the vector control, HA-LARP4B, or HA-LARP4BΔLM. The morphology of the cells was observed on day 5. D, the fold change was calculated on day 5. One-way ANOVA followed by Tukey multiple-comparison *post hoc* test, **, $P < 0.01$; ***, $P < 0.001$. E, HA-tagged proteins were immunoprecipitated from cell extract of LARP4B or LARP4BΔLM-transduced U87MG and U138MG cells. Copurified RNA was isolated and analyzed by qPCR. LARP4B high-ranked targets (*EEF2* and *RALY*) and low-ranked targets (*DDX6* and *TOP2A*) were used as positive and negative control, respectively. Student *t* test, *, $P < 0.05$; **, $P < 0.01$. Data represent mean ± SEM ($n = 3$ per group). Data are representative of two independent experiments.

activity may be involved in LARP4B-mediated growth suppression. To test this possibility, we examined the effect of a p53 knockdown on *LARP4B*-mediated growth suppression by transfecting the dominant-negative form of p53 (p53DN; ref. 25) into the four LARP4B-sensitive glioma cell lines. The proliferation of both p53 wild-type (WT) cell lines (U87MG and A172; refs. 26, 27) was partially rescued by p53DN after *LARP4B* transduction (Fig. 4C and D), indicating that p53 activity is partially required for the LARP4B-mediated growth suppression in these cell lines. In contrast, one of the p53-mutant cell lines (U118MG and U138MG; refs. 26, 27) did not respond to p53DN (Fig. 4C and D), suggesting that the growth-inhibitory effect of LARP4B is p53 mutation-dependent (28).

The RNA-binding ability of LARP4B contributes to its growth-inhibitory function

LARP family proteins are characterized by their La module, which enables the binding of LARP proteins to RNA. To examine whether the La module is essential for the growth-suppressive functions of LARP4B, we created a deletion mutant that lacked the La module (LARP4BΔLM; Fig. 5A and B). Compared with the case with full-length LARP4B, growth suppression was greatly reduced by the deletion of the La module (Fig. 5C and D), indicating that LARP4B inhibits glioma cell growth through an interaction with RNA. As deletion of the La module did not completely rescue LARP4B's growth suppression, LARP4B may also interact with proteins that contribute to the inhibition of glioma cell growth.

LARP4B associates with *BAX* mRNA

A recent study identified RNA targets of LARP4B in HEK293 cells using PAR-CLIP, a transcriptome-wide crosslinking method for RNA-binding proteins (16). *CDKN1A* and *BAX* were included in the list of candidate RNA targets of LARP4B. To validate specific interactions between LARP4B and *CDKN1A* and *BAX* mRNAs, we used RNA immunoprecipitation followed by RT-PCR analysis (RIP-PCR). LARP4B strong targets (*EEF2* and *RALY*) based on a high number of T-to-C transitions (16) showed significantly stronger interactions with LARP4B compared with LARP4BΔLM, whereas such interactions were not observed for weak targets (*DDX6* and *TOP2A*; Fig. 5E). We observed significant interactions between *BAX* mRNA and the La module of LARP4B in both U87MG and U138MG cells, whereas such interactions were observed only in U138MG cells for *CDKN1A* mRNA (Fig. 5E). LARP4B has been shown to stabilize its target mRNAs (16),

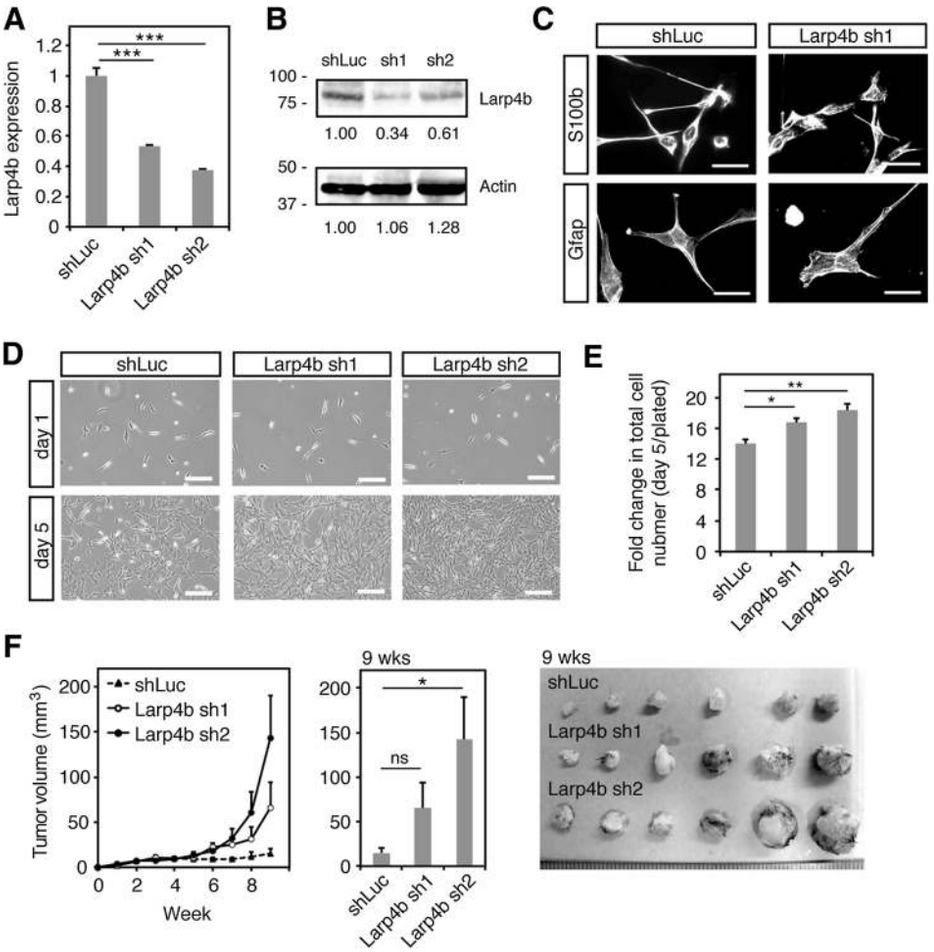

Figure 6.
Larp4b loss promotes tumor formation of primary astrocytes. A, *Larp4b* expression levels in primary astrocytes transfected with shLuc or shRNA against *Larp4b*. Expression levels were normalized by *Gapdh*. B, Western blot analysis of Larp4b expression. Band intensities are indicated. C, expression of astrocyte markers (S100b and Gfap). Scale bars, 50 μm. D, proliferation of primary astrocytes after a *Larp4b* knockdown. Cells were observed on days 1 and 5 after plating. Scale bars, 200 μm. E, fold change was calculated on day 5. Data represent mean ± SEM ($n = 3$ per group). Data are representative of two independent experiments. F, *Larp4b* knockdown promoted subcutaneous tumor formation. Tumor size was monitored until 9 weeks after injection. Millimeter ruler is shown at the bottom. Data represent mean ± SEM ($n = 6$ per group). One-way ANOVA followed by Dunnett multiple-comparison *post hoc* test. *, $P < 0.05$; **, $P < 0.01$; ***, $P < 0.001$.

indicating that a direct interaction between *LARP4B* and *BAX* mRNA may have contributed to *BAX* upregulation.

Larp4b knockdown promoted tumor formation of primary astrocytes

To further confirm the tumor-suppressor function of *Larp4b*, we next examined whether a *Larp4b* knockdown promoted tumor formation. Primary astrocytes were immortalized by p53DN and then retrovirally transduced with shRNA against the *Nf1* tumor-suppressor gene (5), which is frequently mutated in human glioblastoma (29). The p53 and *Nf1*-deficient astrocytes were then infected with a retrovirus that expressed shRNA against *Larp4b*. Decreased expression of *Larp4b* was confirmed by qPCR and Western blot experiments (Fig. 6A and B). Immunostaining confirmed the expression of S100b and Gfap, markers for astrocytes in these cells (Fig. 6C). Analysis of *in vitro* proliferation showed that *Larp4b* silencing increased proliferation of primary astrocytes (Fig. 6D and E). We next analyzed the effects of *Larp4b* knockdown on *in vivo* proliferation. Five million cells were subcutaneously transplanted into C57BL6/J mice. Compared with the control p53 and *Nf1*-deficient astrocytes, the knockdown of *Larp4b* increased the average tumor size (Fig. 6F), although the difference was not significant for sh1. Intracranial injection of these astrocytes revealed EdU incorporation and S100b expression at 2 weeks after transplantation (Supplementary Fig. S4A and S4B). Notably, tumor invasiveness was increased by *Larp4b* knockdown (Supplementary Fig. S4C). After 8 weeks, proliferative lesions were induced by *Larp4b* knockdown (Supplementary Fig. S4D and S4E). The maximal diameter and the cross-sectional area of the lesions were both increased by *Larp4b* knockdown (Supplementary Fig. S4F), although the difference was significant only for sh2. Kaplan–Meier survival analysis revealed that *Larp4b* silencing (sh2) significantly shortened lifespan (Supplementary Fig. S4G). These data indicate that *Larp4b* loss cooperates with the deficiency of p53 and *Nf1* in promoting tumor cell growth.

Discussion

In this study, we identified *LARP4B* as a tumor-suppressor gene in glioma. The pattern of transposon insertions in glioma suggests a tumor-suppressor role for *Larp4b*. Genetic examination of *LARP4B* in human gliomas available in the TCGA database showed that a heterozygous deletion of *LARP4B* is a common event in glioma, supporting the notion that *LARP4B* may function as a tumor suppressor. Importantly, *LARP4B* loss was correlated with decreased *LARP4B* expression, and was negatively correlated

with patient survival, indicating that *LARP4B* loss has a prognostic value.

We found that *Larp4B* has been included as a potential cancer-related candidate gene in other transposon mutagenesis screens, including liver cancer (30), colorectal cancer (31), pancreatic cancer (32), malignant peripheral nerve sheath tumors (33), and medulloblastoma (34), raising the possibility that *Larp4b* is involved in the development of a wide variety of cancers. The patterns of transposon insertions in gastrointestinal tumors (31) and liver cancer (30) support its role as a tumor suppressor (Supplementary Fig. S5A and S5B). A recent study used shRNA to almost completely knockdown endogenous *Larp4b* in leukemia stem cells and found that proliferation was impaired (35), which is in contrast to our finding that decreased *Larp4b* levels promoted proliferation of primary astrocytes as well as tumor formation. The discrepancy between these phenotypes may be explained by the idea that a certain *Larp4b* expression level is critical, and complete depletion of *Larp4b* might be toxic, even to cancer cells. Another possibility is that Larp4b may function differentially in different types of cancer. In fact, transposon mutagenesis screens have identified *Larp4b* as a candidate cancer gene for many types of solid tumors (5, 30–34); however, *Larp4b* has not been identified in acute myeloid leukemia (AML; ref. 36). Moreover, *LARP4B* is diploid in approximately 98% of human AML cases (Supplementary Table S7), supporting the notion that LARP4B does not act as a tumor suppressor in AML.

LARP4B transduction induced strong growth suppression in several glioma cell lines; however, such growth suppression was moderate for U251MG glioma cells, and T98G continued to proliferate even after LARP4B transduction. This difference cannot be explained by differential expression of endogenous *LARP4B* in glioma lines, as *LARP4B* expression levels in glioma lines were not correlated with the growth-inhibitory effects of LARP4B. A possible cause for this resistance may be defects in the molecular mechanisms regulating mitotic arrest and apoptosis, by either genetic or epigenetic alterations. We found that p53 activity was partially responsible for the growth-suppressive effects of LARP4B in p53 WT cells lines; however, p53 status alone is not sufficient to explain the difference in phenotype because the LARP4B-sensitive cell lines U118MG and U138MG express mutant p53 (26, 27). A previous study showed that *CDKN1A* ($p21^{CIP1}$) induction was responsible for the differential response of glioma cell lines to TGFβ-mediated growth suppression (37). The U87MG line is sensitive to TGFβ by inducing *CDKN1A* expression; however, the T98G and U251MG lines are not sensitive to TGFβ because *CDKN1A* induction does not occur in these glioma cell lines (37). Notably, T98G and U251MG are less sensitive to LARP4B than the other four lines, and most of the glioma lines that are sensitive to LARP4B expressed *CDKN1A* at high levels, supporting the notion that *CDKN1A* induction is responsible for the difference in the response of glioma cell lines to LARP4B.

The LARP4B-mediated growth suppression was partially rescued by p53DN; however, the rescue effect was quite modest even in p53 WT cell lines, indicating that LARP4B is acting mainly through p53-independent pathways. We found that the RNA-binding ability of LARP4B contributed to its growth-inhibitory function, indicating that LARP4B suppresses glioma cell growth through an interaction with RNA. Deregulated expression of RNA-binding proteins is commonly observed in cancer (38), and emerging evidence indicates causative roles for the dysregulation of RNA-binding proteins in cancer progression (39). Alternative splicing of mRNA precursors (pre-mRNA) is one of the mechanisms through which dysregulation of RNA-binding proteins confers growth advantage to cancer cells, because cancer cells favor the production of protein isoforms that promote growth and survival (17, 40). Another mechanism through which RNA-binding proteins regulate cancer progression involves changes in mRNA stability (41). A recent transcriptome-wide analysis of LARP4B target genes showed that LARP4B binds mainly to mature mRNAs at their 3′ untranslated regions, resulting in stabilization of the target mRNAs at the posttranscriptional level with corresponding changes in protein levels (16). As we observed a direct interaction between LARP4B and *BAX* mRNA, LARP4B transduction may have stabilized *BAX* mRNA, which in turn caused apoptotic phenotypes in glioma cells. Interestingly, we observed cell-type–specific interactions between LARP4B and *CDKN1A* mRNA, which can be explained by the difference in expression levels of other interacting proteins, as PABPC1, an LARP4B-interacting partner (13), serves as a scaffold for those proteins, including PAN3, PAIP1, PAIP2, and TNRC6A, which influence the stabilization of mRNAs (42).

In addition to *BAX*, the PAR-CLIP experiment identified a large number of RNA targets of LARP4B in HEK293 cells (16). A Gene Ontology term enrichment analysis of the top 100 genes ranked by the number of T-to-C transitions identified biologic processes associated with translation ($P = 3.7 \times 10^{-5}$) and RNA splicing ($P = 6.5 \times 10^{-5}$) as being highly significant; however, pathways associated with cell-cycle regulation and apoptosis were not identified. Kuspert and colleagues used full-length LARP4B for the PAR-CLIP experiment (16), suggesting that some RNAs identified in their study interacted with LARP4B at regions outside the La module. As the La module is essential for the growth-inhibitory effect of LARP4B, identification of the RNA targets of LARP4B specifically associated with the La module would provide important insight into the mechanisms through which LARP4B induces growth inhibition in glioma.

Disclosure of Potential Conflicts of Interest

No potential conflicts of interest were disclosed.

Authors' Contributions

Conception and design: H. Koso, H. Yi, S. Watanabe
Development of methodology: H. Koso, H. Yi
Acquisition of data (provided animals, acquired and managed patients, provided facilities, etc.): H. Koso, H. Yi, T. Todo
Analysis and interpretation of data (e.g., statistical analysis, biostatistics, computational analysis): H. Koso, H. Yi, P. Sheridan, S. Miyano
Writing, review, and/or revision of the manuscript: H. Koso, H. Yi, P. Sheridan, S. Watanabe
Administrative, technical, or material support (i.e., reporting or organizing data, constructing databases): H. Yi, Y. Ino
Study supervision: S. Watanabe

Acknowledgments

The authors thank Eli Lyons for supporting Yi's experiments.

Grant Support

This work was supported by the Japan Society for the Promotion of Science.

The costs of publication of this article were defrayed in part by the payment of page charges. This article must therefore be hereby marked *advertisement* in accordance with 18 U.S.C. Section 1734 solely to indicate this fact.

Received August 20, 2015; revised February 10, 2016; accepted February 17, 2016; published OnlineFirst March 1, 2016.

References

1. Ohgaki H, Kleihues P. Epidemiology and etiology of gliomas. Acta Neuropathol 2005;109:93–108.
2. Brennan CW, Verhaak RG, McKenna A, Campos B, Noushmehr H, Salama SR, et al. The somatic genomic landscape of glioblastoma. Cell 2013; 155:462–77.
3. Copeland NG, Jenkins NA. Harnessing transposons for cancer gene discovery. Nat Rev Cancer 2010;10:696–706.
4. DeNicola GM, Karreth FA, Adams DJ, Wong CC. The utility of transposon mutagenesis for cancer studies in the era of genome editing. Genome Biol 2015;16:229.
5. Koso H, Takeda H, Yew CC, Ward JM, Nariai N, Ueno K, et al. Transposon mutagenesis identifies genes that transform neural stem cells into glioma-initiating cells. Proc Natl Acad Sci U S A 2012;109:E2998–3007.
6. Alfano C, Sanfelice D, Babon J, Kelly G, Jacks A, Curry S, et al. Structural analysis of cooperative RNA binding by the La motif and central RRM domain of human La protein. Nat Struct Mol Biol 2004;11:323–9.
7. Wolin SL, Cedervall T. The La protein. Annu Rev Biochem 2002;71: 375–403.
8. Stavraka C, Blagden S. The La-Related proteins, a family with connections to cancer. Biomolecules 2015;5:2701–22.
9. Diribarne G, Bensaude O. 7SK RNA, a non-coding RNA regulating P-TEFb, a general transcription factor. RNA Biol 2009;6:122–8.
10. Markert A, Grimm M, Martinez J, Wiesner J, Meyerhans A, Meyuhas O, et al. The La-related protein LARP7 is a component of the 7SK ribonucleoprotein and affects transcription of cellular and viral polymerase II genes. EMBO Rep 2008;9:569–75.
11. Cheng Y, Jin Z, Agarwal R, Ma K, Yang J, Ibrahim S, et al. LARP7 is a potential tumor suppressor gene in gastric cancer. Lab Invest 2012;92: 1013–9.
12. Ji X, Lu H, Zhou Q, Luo K. LARP7 suppresses P-TEFb activity to inhibit breast cancer progression and metastasis. Elife 2014;3:e02907.
13. Schäffler K, Schulz K, Hirmer A, Wiesner J, Grimm M, Sickmann A, et al. A stimulatory role for the La-related protein 4B in translation. Rna 2010; 16:1488–99.
14. Ikushima H, Todo T, Ino Y, Takahashi M, Miyazawa K, Miyazono K. Autocrine TGF-beta signaling maintains tumorigenicity of glioma-initiating cells through Sry-related HMG-box factors. Cell Stem Cell 2009;5:504–14.
15. Koso H, Tsuhako A, Lyons E, Ward JM, Rust AG, Adams DJ, et al. Identification of FoxR2 as an oncogene in medulloblastoma. Cancer Res 2014;74:2351–61.
16. Küspert M, Murakawa Y, Schäffler K, Vanselow JT, Wolf E, Juranek S, et al. LARP4B is an AU-rich sequence associated factor that promotes mRNA accumulation and translation. Rna 2015;21:1294–305.
17. Zong FY, Fu X, Wei WJ, Luo YG, Heiner M, Cao LJ, et al. The RNA-binding protein QKI suppresses cancer-associated aberrant splicing. PLoS Genet 2014;10:e1004289.
18. Chen AJ, Paik JH, Zhang H, Shukla SA, Mortensen R, Hu J, et al. STAR RNA-binding protein Quaking suppresses cancer via stabilization of specific miRNA. Genes Dev 2012;26:1459–72.
19. Razak SR, Ueno K, Takayama N, Nariai N, Nagasaki M, Saito R, et al. Profiling of microRNA in human and mouse ES and iPS cells reveals overlapping but distinct microRNA expression patterns. PLoS One 2013;8: e73532.
20. Rodier F, Campisi J. Four faces of cellular senescence. J Cell Biol 2011;192:547–56.
21. Hall LL, Th'ng JP, Guo XW, Teplitz RL, Bradbury EM. A brief staurosporine treatment of mitotic cells triggers premature exit from mitosis and polyploid cell formation. Cancer Res 1996;56:3551–9.
22. Malumbres M, Barbacid M. Cell cycle, CDKs and cancer: A changing paradigm. Nat Rev Cancer 2009;9:153–66.
23. Westphal D, Kluck RM, Dewson G. Building blocks of the apoptotic pore: How Bax and Bak are activated and oligomerize during apoptosis. Cell Death Differ 2014;21:196–205.
24. Khoo KH, Verma CS, Lane DP. Drugging the p53 pathway: Understanding the route to clinical efficacy. Nat Rev Drug Discov 2014; 13:217–36.
25. Shaulian E, Zauberman A, Ginsberg D, Oren M. Identification of a minimal transforming domain of p53: Negative dominance through abrogation of sequence-specific DNA binding. Mol Cell Biol 1992;12: 5581–92.
26. Batista LF, Roos WP, Christmann M, Menck CF, Kaina B. Differential sensitivity of malignant glioma cells to methylating and chloroethylating anticancer drugs: p53 determines the switch by regulating xpc, ddb2, and DNA double-strand breaks. Cancer Res 2007;67:11886–95.
27. Alonso M, Tamasdan C, Miller DC, Newcomb EW. Flavopiridol induces apoptosis in glioma cell lines independent of retinoblastoma and p53 tumor suppressor pathway alterations by a caspase-independent pathway. Mol Cancer Ther 2003;2:139–50.
28. Muller PA, Vousden KH. p53 mutations in cancer. Nat Cell Biol 2013;15:2–8.
29. Verhaak RG, Hoadley KA, Purdom E, Wang V, Qi Y, Wilkerson MD, et al. Integrated genomic analysis identifies clinically relevant subtypes of glioblastoma characterized by abnormalities in PDGFRA, IDH1, EGFR, and NF1. Cancer Cell 2010;17:98–110.
30. Bard-Chapeau EA, Nguyen AT, Rust AG, Sayadi A, Lee P, Chua BQ, et al. Transposon mutagenesis identifies genes driving hepatocellular carcinoma in a chronic hepatitis B mouse model. Nat Genet 2014;46:24–32.
31. Takeda H, Wei Z, Koso H, Rust AG, Yew CC, Mann MB, et al. Transposon mutagenesis identifies genes and evolutionary forces driving gastrointestinal tract tumor progression. Nat Genet 2015;47:142–50.
32. Pérez-Mancera PA, Rust AG, van der Weyden L, Kristiansen G, Li A, Sarver AL, et al. The deubiquitinase USP9X suppresses pancreatic ductal adenocarcinoma. Nature 2012;486:266–70.
33. Rahrmann EP, Watson AL, Keng VW, Choi K, Moriarity BS, Beckmann DA, et al. Forward genetic screen for malignant peripheral nerve sheath tumor formation identifies new genes and pathways driving tumorigenesis. Nat Genet 2013;45:756–66.
34. Wu X, Northcott PA, Dubuc A, Dupuy AJ, Shih DJ, Witt H, et al. Clonal selection drives genetic divergence of metastatic medulloblastoma. Nature 2012;482:529–33.
35. Zhang Y, Peng L, Hu T, Wan Y, Ren Y, Zhang J, et al. La-related protein 4B maintains murine MLL-AF9 leukemia stem cell self-renewal by regulating cell cycle progression. Exp Hematol 2015;43:309–18 e2.
36. Vassiliou GS, Cooper JL, Rad R, Li J, Rice S, Uren A, et al. Mutant nucleophosmin and cooperating pathways drive leukemia initiation and progression in mice. Nat Genet 2011;43:470–5.
37. Rich JN, Zhang M, Datto MB, Bigner DD, Wang XF. Transforming growth factor-beta-mediated p15(INK4B) induction and growth inhibition in astrocytes is SMAD3-dependent and a pathway prominently altered in human glioma cell lines. J Biol Chem 1999;274:35053–8.
38. Kechavarzi B, Janga SC. Dissecting the expression landscape of RNA-binding proteins in human cancers. Genome Biol 2014;15:R14.
39. Kim MY, Hur J, Jeong S. Emerging roles of RNA and RNA-binding protein network in cancer cells. BMB Rep 2009;42:125–30.
40. David CJ, Manley JL. Alternative pre-mRNA splicing regulation in cancer: Pathways and programs unhinged. Genes Dev 2010;24:2343–64.
41. Vanharanta S, Marney CB, Shu W, Valiente M, Zou Y, Mele A, et al. Loss of the multifunctional RNA-binding protein RBM47 as a source of selectable metastatic traits in breast cancer. Elife 2014;3.
42. Jonas S, Izaurralde E. Towards a molecular understanding of microRNA-mediated gene silencing. Nat Rev Genet 2015;16:421–33.